Model error estimation for the CPTEC Eta model*

Michael K. Tippett† Arlindo da Silva‡

May 26, 1999

Abstract

Statistical data assimilation systems require the specification of forecast and observation error statistics. Forecast error is due to model imperfections and differences between the initial condition and the actual state of the atmosphere. Practical four-dimensional variational (4D-Var) methods try to fit the forecast state to the observations and assume that the model error is negligible. Here with a number of simplifying assumption, a framework is developed for isolating the model error given the forecast error at two lead-times. Two definitions are proposed for the Talagrand ratio τ, the fraction of the forecast error due to model error rather than initial condition error. Data from the CPTEC Eta Model running operationally over South America are used to calculate forecast error statistics and lower bounds for τ.

1 Introduction

Data assimilation systems combine satellite data and other measurements with a first guess coming from a predictive model to produce an analysis or estimate of the state of the atmosphere. This estimate can be used as an initial condition for numerical weather prediction, or a sequence of estimates can be used to study Earth Science phenomena. In statistical data assimilation methods the analysis is a weighted average of the model forecast and current observations. The weighting is determined by the specification of forecast and observation error statistics. For instance, where forecast error is large, more weight is given to observations. Forecast error statistics also determine how observations correct forecast errors in a neighborhood of the observation.

*This work was supported by Conselho Nacional de Desenvolvimento Científico e Tecnológico (CNPq) Grant 381737/97-7, Fundação de Amparo à Pesquisa do Estado de São Paulo (FAPESP) Grant 1998/11952-0 and the NASA EOS Interdisciplinary Project on Data Assimilation.

†International Research Institute for climate prediction, Lamont-Doherty Earth Observatory of Columbia University, Palisades, NY 10964-8000, USA (tippett@iri.ldgo.columbia.edu). This work was done while the author was with the Centro de Previsão de Tempo e Estudos Climáticos, Cachoeira Paulista, SP, Brazil.

‡Data Assimilation Office, Code 910.3, NASA/GSFC, Greenbelt, MD 20771, USA (dasilva@dao.gsfc.nasa.gov).

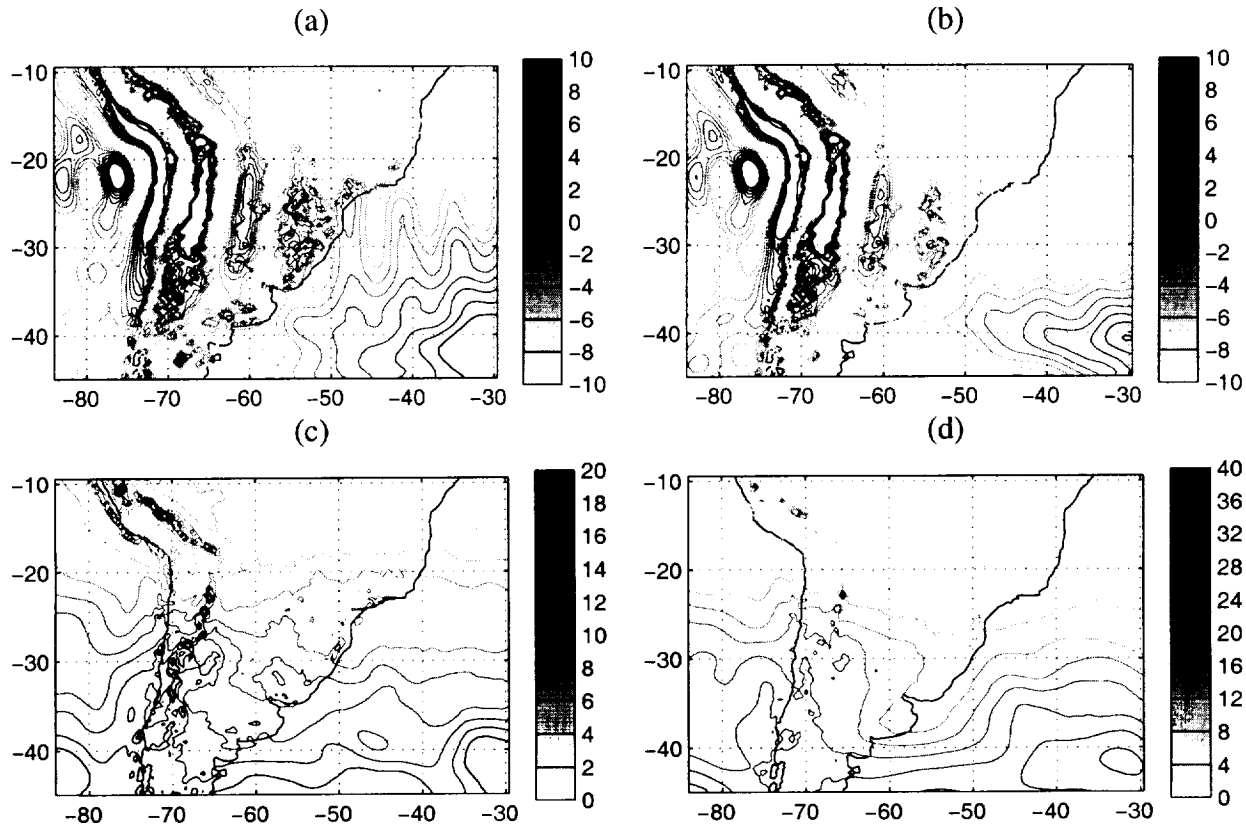

Figure 1: Contour plots at 500 mb of the forecast height error bias at (a) 24 hours (b) 48 hours and of the forecast height error standard deviation at (c) 24 hours and at (d) 48 hours; units are meters.

and 12 UTC. The CPTEC Eta Model forecast error is approximated by the difference of the forecast and the NCEP operational analysis. We note that quality of the 0Z and 12Z NCEP analyses is likely different since the number of observations is greater at 12Z. The NCEP analysis, interpolated onto the Eta grid, is also the initial condition for the operational CPTEC Eta model. We calculate forecast error statistics for the period during August of 1998 using a subset of the complete set of predicted variables, namely the height fields at three levels 300, 500 and 700 mb on the region 85W to 30W and 45S to 10S interpolated onto a $0.4^\circ \times 0.4^\circ$ grid. The forecast error mean and standard deviation are shown at the 500 mb level in Fig. 1.

Much of the systematic difference between forecast and analysis is related to the spectral topography representation of the analysis. The spectral topography of the NCEP analysis is very different from the mountain-step coordinate representation of the Eta model near the Andes. The resulting NCEP analysis fields when interpolated onto the Eta model grid are incompatable with the Eta model topography. Features in the western part of the domain are independent of the forecast lead-time while systematic differences between Eta forecast and NCEP analysis over the

2 Methodology

In the context of linear dynamics, we can obtain the model error covariance given the forecast error covariances at two lead-times, for instance given the 24-hour and 48-hour forecast error covariances. Define forecast error $\epsilon_{k;k+1}$ to be the error of the forecast starting at time k and valid at time $k+1$. We use time-steps of 24-hours. The 24-hour forecast error $\epsilon_{k;k+1}$ is the difference at time $k+1$ of the 24-hour forecast and the true state w^t_{k+1},

$$\epsilon_{k;k+1} = \mathbf{M}_{k;k+1} w^a_k - w^t_{k+1}\,; \tag{1}$$

w^a_k is the analysis at time k and $\mathbf{M}_{k;k+1}$ is the linear operator that advances the state from time k to time $k+1$. Likewise, define the 48-hour forecast error $\epsilon_{k;k+2}$ to be the difference of the 48-hour forecast and the true state w^t_{k+2} at time $k+2$,

$$\epsilon_{k;k+2} = \mathbf{M}_{k;k+2} w^a_k - w^t_{k+2}\,. \tag{2}$$

The 48-hour forecast error is due to the propagated 24-hour forecast error and the model error as shown by

$$\begin{aligned} \epsilon_{k;k+2} &= \mathbf{M}_{k;k+2} w^a_k - w^t_{k+2} = \mathbf{M}_{k+1;k+2}(\mathbf{M}_{k;k+1} w^a_k - w^t_{k+1}) - \epsilon^t_{k+2} \\ &= \mathbf{M}_{k+1;k+2}\epsilon_{k;k+1} - \epsilon^t_{k+2}\,. \end{aligned} \tag{3}$$

The model error ϵ^t_{k+1} is defined by

$$\epsilon^t_{k+1} = w^t_{k+1} - \mathbf{M}_{k;k+1} w^t_k\,. \tag{4}$$

The 24-hour and 48-hour forecast error covariances $\mathbf{P}_{k;k+1}$ and $\mathbf{P}_{k;k+2}$ satisfy

$$\mathbf{P}_{k;k+2} \equiv \left\langle \epsilon_{k;k+2}\epsilon^T_{k;k+2} \right\rangle = \mathbf{M}_{k+1;k+2}\mathbf{P}_{k;k+1}\mathbf{M}^T_{k+1;k+2} + \mathbf{Q}_{k+1}\,, \tag{5}$$

where we have taken $\left\langle \epsilon^t_k (\epsilon^t_k)^T \right\rangle = \mathbf{Q}_k$; we use the notation $\langle\cdot\rangle$ to denote ensemble average. Therefore, the model error covariance $\mathbf{Q}_{k+1}$ can be obtained given the dynamics $\mathbf{M}_{k+1:k+2}$ and the forecast error covariances $\mathbf{P}_{k;k+1}$ and $\mathbf{P}_{k;k+2}$.

There are difficulties with the method presented above. First, the true state, and hence the forecast error, is unknown. Therefore, we make the approximation of replacing the true state by the verifying analysis, i.e., instead of (1) we take

$$\epsilon_{k;k+1} = \mathbf{M}_{k;k+1} w^a_k - w^a_{k+1}\,. \tag{6}$$

Another lower bound for $\tau_{\rm var}$ depends on the variance $\lambda_1(\mathbf{P}_{24})$ associated with the leading eigenvector of the 24 hour forecast error covariance and the quantity $\mathrm{tr}\,\mathbf{M}\mathbf{M}^T$, namely:

$$\tau_{\rm var} \geq 1 - \frac{\lambda_1(\mathbf{P}_{24})}{\mathrm{tr}\,\mathbf{P}_{48}}\,\mathrm{tr}(\mathbf{M}\mathbf{M}^T)\,. \tag{10}$$

This lower bound reflects a worse-case situation where spectrum of the 24 hour forecast error covariance is flat. Recall that

$$\mathrm{tr}\,\mathbf{M}\mathbf{M}^T = \sum_{i=1}^{n} \sigma_i^2(\mathbf{M})\,, \tag{11}$$

and is the expected amplification of the variance of an uncorrelated, homogeneous random initial condition (Tippett 1999). Therefore, given the singular values of $\mathbf{M}$ and the eigenvalues of the 24 and 48 hour forecast error covariance, lower bounds for $\tau_{\rm var}$ can be obtained.

Another measure of the model error is the volume Talagrand ratio $\tau_{\rm vol}$ defined as (Schneider & Griffies 1999)

$$\tau_{\rm vol} = \left(\frac{\det\mathbf{Q}}{\det\mathbf{P}_{48}}\right)^{1/n} = \left(\frac{\det\left(\mathbf{P}_{48} - \mathbf{M}\mathbf{P}_{24}\mathbf{M}^T\right)}{\det\mathbf{P}_{48}}\right)^{1/n}\,; \tag{12}$$

n is the dimension of the state-space. This definition has the following geometric interpretation. For a Gaussian random variable with zero mean and covariance $\mathbf{P}$, the ellipsoid $\mathcal{E}_p(\mathbf{P})$ that encloses some fraction $0 < p < 1$ of the cumulative probability distribution has a volume proportional to $(\det\mathbf{P})^{1/2}$. Therefore, the Talagrand ratio $\tau_{\rm vol}$ is the square of the geometric mean of the semiaxis lengths of the model error ellipsoid $\mathcal{E}_p(\mathbf{Q})$ over the square of the geometric mean of the semiaxis lengths of the 48-hour forecast error ellipsoid $\mathcal{E}_p(\mathbf{Q})$. We note that this definition is invariant under general nonsingular transformations of the state-space. As a consequence, $\tau_{\rm vol}$ does not depend on the choice of inner product. A lower bound for $\tau_{\rm vol}$ is

$$\tau_{\rm vol} \geq 1 - \left((\det\mathbf{M})^2\,\frac{\det\mathbf{P}_{24}}{\det\mathbf{P}_{48}}\right)^{1/n}\,. \tag{13}$$

Special care in calculating $\tau_{\rm vol}$ must be taken when the covariance or dynamics matrices are singular. The simplest remedy and the one we use here is to compute the determinants on a reduced spaces where the matrices are nonsingular.

In Fig. 3 we plot lower bounds for $\tau_{\rm var}$ and $\tau_{\rm vol}$ as function of the singular values of the dynamics for the approximate forecast error covariance matrices calculated here for the Eta model. If the model dynamics does not amplify the 24-hour forecast error, the 48-hour forecast error is due

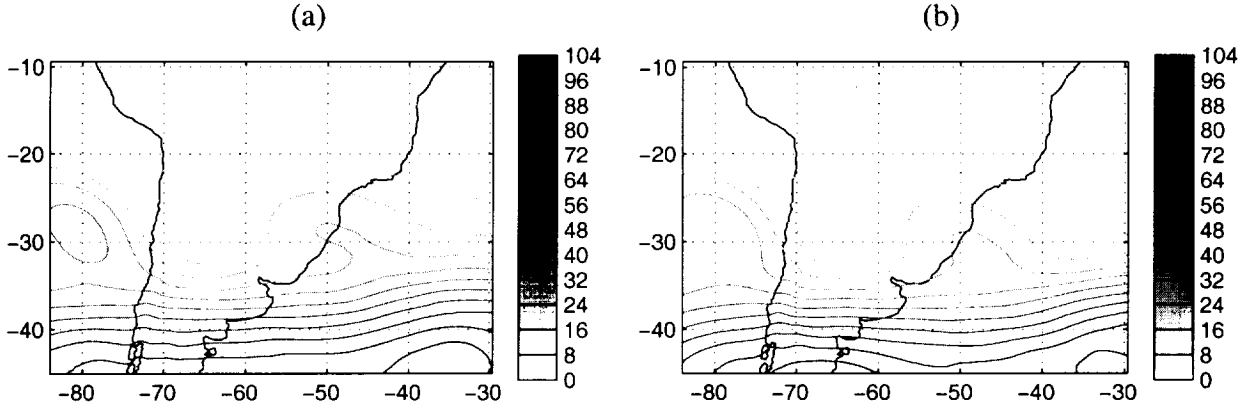

Figure 4: The standard deviations of the (a) 24-hour and (b) 48-hour forecast anomaly height fields plotted at 500 mb. Units are meters

modes associated with small eigenvalues are likely to suffer from sampling error. On the other hand, keeping too few modes produces dynamics that does not produce growth. Here we choose to retain 5 modes of $\mathbf{P}_{24}^{f}$ explaining 85% of its total variance. Later we show how the lower bounds for τ depend on the number of modes retained.

Figure 4 shows the standard deviation of the 24 and 48 hour forecast height anomaly fields. As expected there are only slight differences between the standard deviation of the 24 and 48 hour height anomaly fields; both should approximate the natural variability of the height field during this period. The variability of the model may be different from the model error. For instance, model error may be a results of the model not presenting the same variability seen in nature. However, there are some similarities between the two here. Model error is much noisier. Calculation of the principle angles show that the leading eigenmodes of $\mathbf{P}_{24}^{f}$ and $\mathbf{P}_{48}^{f}$ span approximately the same subspaces.

Figure 5(a) shows the singular values of $\mathbf{M}$. Although the dynamics is stable by construction with all eigenvalues inside the unit circle, there are singular values greater than one, indicating nonmodal growth. Figure 5(b) shows the extent to which the Markov model dynamics is able to propagate the 24 hour forecast height anomaly. The deterministic part of the signal is not substantially larger than the random component. The covariance of the residual $\langle bb^T \rangle$ is computed in the full-space and is larger than the truncated part of the anomaly covariances.

Figure 6 shows the leading right and left singular vectors of $\mathbf{M}$. Their structure is related to the entrance of fronts and cyclogenesis in the Atlantic; 9 fronts passed through the region during the period. Using the singular values of the Markov model $\mathbf{M}$ in (9) and (10) gives as lower bound for

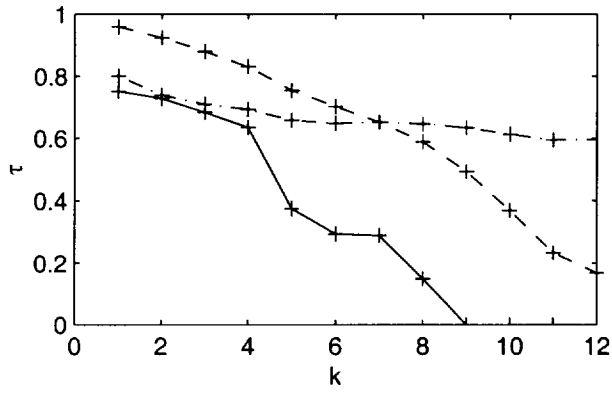

Figure 7: The lower bounds in Eq. (9) (solid line), Eq. (10) (dashed line) and Eq. (13) (dotted dashed line) as function of the number k of modes used in the Markov model calculation.

the Talagrand ratio $\tau_{\text{var}} \geq 0.37$ and $\tau_{\text{var}} \geq 0.76$ respectively; (13) gives $\tau_{\text{vol}} \geq 0.70$ where we have conservatively used only 3 modes to compute determinants. Using more modes in the calculation of the Markov dynamics increases the singular values and decreases the lower bound as shown in Fig. 7. Of the three lower bounds, (9) is the most sensitive to the number of modes retained since it depends only on the size of the largest singular value $\sigma_1(\mathbf{M})$ of $\mathbf{M}$.

The lower bounds for τ come from assuming that the 24-hour errors project favorably onto the growing modes of the dynamics. However, the dimension of both the subspace of dominant forecast errors and of the subspace of dynamically growing modes, around 10, is small compared to the dimension of the full space 36,990. The likelihood that two arbitrarily chosen subspaces intersect is therefore small. We first compare the subspaces spanned by the forecast errors and by the forecast anomalies by comparing their principle angles (see Appendix). Figure 8 shows that there is reasonable correspondence between the subspaces spanned by the forecast error and the forecast anomaly. The correspondence is less at 48-hours than at 24 hours. At both lead times there are principle angles of about 80° indicating that there are forecast errors that project very weakly onto the subspace spanned by the forecast anomaly.

For the forecast anomaly dynamics to be able to amplify efficiently 24-hour forecast errors into 48-hour forecast errors, there must be a favorable relationship between the leading subspaces of the error covariance and the singular vectors of the dynamics. Namely, the 24-hour forecast errors must project onto the leading right singular vectors of the dynamics and the 48-hour forecast errors must project onto the left singular vectors of the dynamics. In Fig. 9 we compare the subspaces spanned by the errors and by the singular vectors of the Markov model. In Fig. 9(a) we observed that the

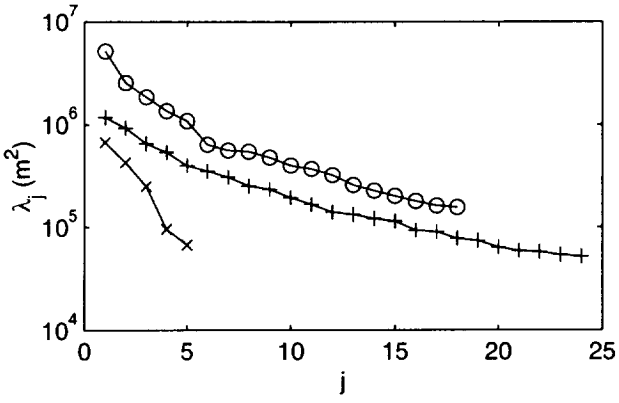

Figure 10: As in Fig. 2 with the addition of the eigenvalues of $\mathbf{MP}_{24}\mathbf{M}^T$ (solid line with x's).

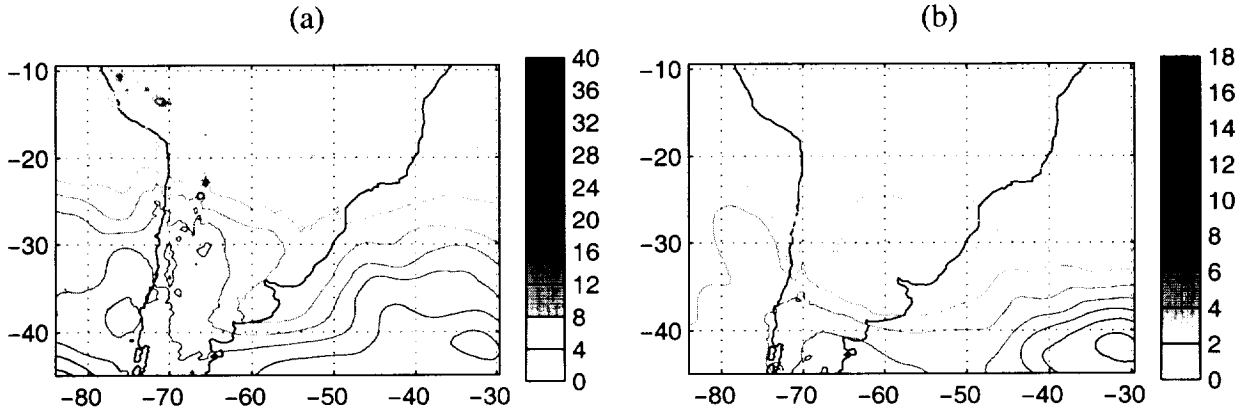

Figure 11: Contour plots of the standard deviation of (a) $\mathbf{Q}$ and (b) $\mathbf{MP}_{24}\mathbf{M}^T$ shown at 500 mb. Units are meters.

Figure 11 where the standard deviation of $\mathbf{Q}$ and $\mathbf{MP}_{24}\mathbf{M}^T$ are shown demonstrates that the model error dominates the propagated forecast error and is little different from the 48-hour forecast error.

4 Concluding Remarks

Characterization of prediction model error is important for understanding the performance of data assimilation systems. Advanced sequential data assimilation methods capable of calculating the propagated analysis error require specification of the model error. 4D-Var adjoint methods assume that the model error is negligible.

A measure of the relative size of the model error is the Talagrand ratio τ, the fraction of the forecast error due to model error. We have proposed two definitions for τ. The first is simply the ratio of the model error variance to forecast error variance; the underlying norm is the RMS one.

References

Bennett, A. F. (1992). *Inverse Methods in Physical Oceanography*. Cambridge University Press.

Black, T. L. (1994). The new NMC mesoscale eta model: Description and forecast examples, *Wea. Forecasting* **9**, 265–278.

Chou, S. C. (1996). Model Regional Eta, *Climanálise* .

Cohn, S. E. (1997). An Introduction to Estimation Theory, *J. Meteor. Soc. Japan* **75**, 257–288.

Dee, D. P. (1995). On-line estimation of error covariance parameters for atmospheric data assimilation, *Mon. Wea. Rev.* **123**, 1128–1145.

Ehrendorfer (1994). The Liouville equation and its potential usefulness for the prediction of forecast skill. Part I Theory, *Mon. Wea. Rev.* **122**, 703–713.

Ehrendorfer, M. & Tribbia, J. (1997). Optimal Prediction of Forecast Error Covariances through Singular Vectors, *J. Atmos. Sci.* **54**, 286–313.

Epstein, E. S. (1969). Stochastic Dynamic Prediction, *Tellus* **21**, 739–759.

Farrell, B. F. (1990). Small Error Dynamics and the Predictability of Atmospheric Flows, *J. Atmos. Sci.* **47**, 2409–2416.

Ghil, M. & Malanotte-Rizzoli, P. (1991), *Advances in Geophysics*, Vol. 33, Academic Press, chapter Data assimilation in meteorology and oceanography, pp. 141–266.

Golub, G. H. & Van Loan, C. F. (1996). *Matrix Computations*. Third edn, The Johns Hopkins University Press, Baltimore. 694 pp.

Gustafsson, N., Källén, E. & Thorsteinsson, S. (1998). Sensitivity of forecast errors to initial and lateral boundary conditions, *Tellus* **50A**, 167–185.

Houtekamer, P. L. & Mitchell, H. L. (1998). Data Assimilation Using an Ensemble Kalman Filter Technique, *Mon. Wea. Rev.* **126**, 796–811.

Leith, C. E. (1974). Theoretical skill of Monte Carlo forecasts, *Mon. Wea. Rev.* **102**, 409–418.